JET–P(97)50

Electron and Neutral Interactions with Impurities in Divertor Plasma

H P Summers[1], H Anderson[1], N R Badnell[1], F Bliek[2], M Brix[3], F J de Heer[2], R Hoekstra[2], D C Griffin[4], L D Horton, C F Maggi, M G O'Mullane[1], M Z Pindzola[5].

JET Joint Undertaking, Abingdon, Oxfordshire, OX14 3EA,

[1] Department of Physics and Applied Physics, University of Strathclyde, Glasgow, G4 0NG, UK.

[2] KVI, Atomic Physics, Zernikelaan 25, 9747 AA Groningen, The Netherlands.

[3] Institut für Plasmaphysik, Forschungszentrum Jülich GmbH, EURATOM Association, Trilateral Eurgio Cluster, D-52425 Jülich, Germany.

[4] Department of Physics, Rollins College, Winter Park, Florida 32789 USA.

[5] Department of Physics, Auburn University, Auburn, Alabama 36849 USA.

Preprint of a Paper to be submitted for publication in a Book of Invited Talks of the Atomic Data Sub-meeting of 6th International Workshop on Plasma Edge Theory in Fusion Devices, Exeter College, Oxford, UK, 18 September 1997.

December 1997

Electron and neutral interactions with impurities in divertor plasma

H P Summers†, H Anderson†, N R Badnell†, F Bliek§, M Brix¶, F J de Heer§, R Hoekstra§, D C Griffin♭, L D Horton‡, C F Maggi‡, M G O'Mullane† and M S Pindzola♮

† Department of Physics and Applied Physics, University of Strathclyde, Glasgow G4 0NG, UK

‡ JET Joint Undertaking, Abingdon, Oxon. OX14 3EA, UK

§ KVI, Atomic Physics, Zernikelaan 25, 9747 AA Groningen , Netherlands

¶ Institut fuer Plasmaphysik, Forschungszentrum Juelich GmbH, EURATOM Association, Trilateral Euregio Cluster, D-52425 Juelich Germany

♭ Department of Physics, Rollins College, Winter Park, Florida 32789 USA

♮ Department of Physics, Auburn University,Auburn, Alabama 36849 USA

Abstract.

With the current focus on the characteristics and effective operation of divertor configurations in fusion plasma research, reassessment of the atomic data base available for divertor modelling and diagnosis is taking place. The quest for ideal materials for divertor targets and for impurities which can be used to promote optimum working conditions has exposed some gaps in the database. Equally, for the finer spectroscopic diagnostic and modelling tools now being promoted, existing data may be organised inappropriately or may be at unsuitable precisions. In the present paper, some examples, which emphasise electron collisions and collisions with neutrals, are used to demonstrate these points. Then a case study is presented, based on experience at JET Joint Undertaking, of tailoring atomic data and its manipulation for experiment support.

PACS numbers: 52.55, 52.70

Short title: Electron and neutral interactions with impurities in divertor plasma

October 15, 1997

1. Introduction

Over the last eight years implementation of the axi-symmetric poloidal divertor concept on the JET machine has led to extensive redesigning of the vessel interior and magnetic field coils to produce appropriate magnetic null (X-point) positions, connection lengths and divertor target tiles for the plasma flowing down the scrape-off-layer. Experimental campaigns have investigated the properties of the Mk1 and Mk2A designs. The next stage in this evolution is the Mk2GB (gas box) design due for installation at the end of 1997.

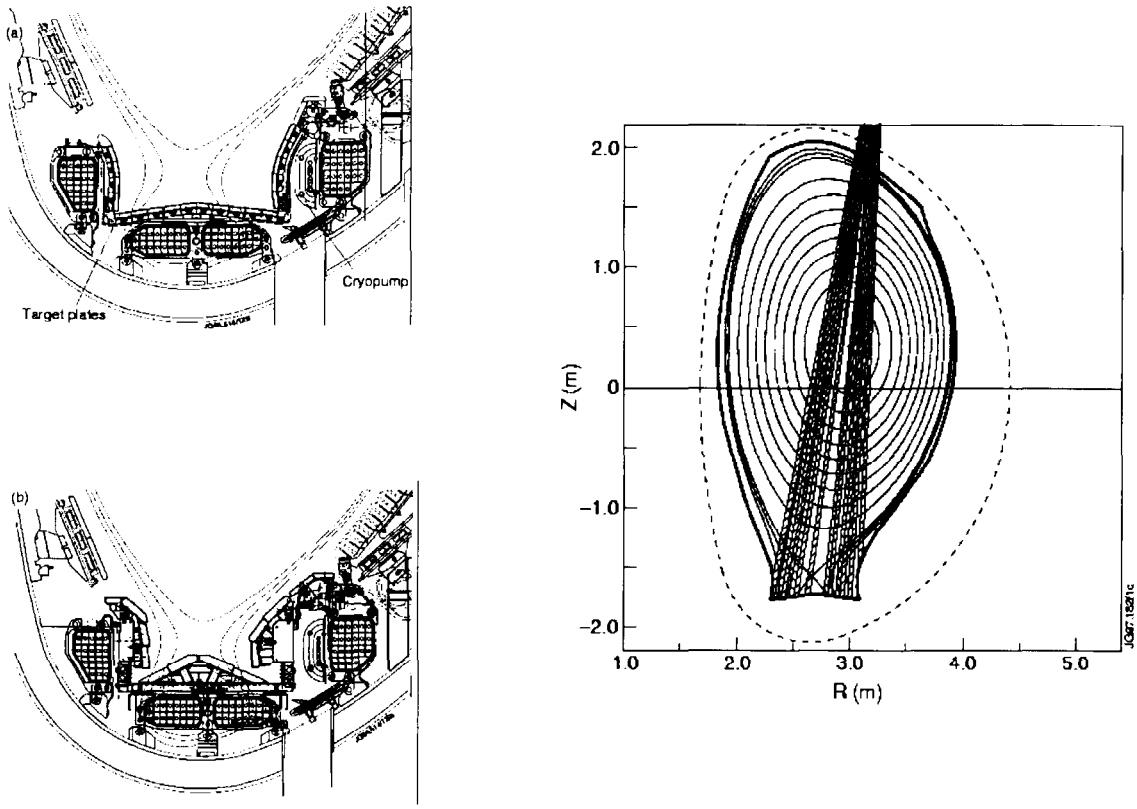

Figure 1. (a) Schematic poloidal section of the JET torus showing the geometrical arrangement of the coils and target plates of the JET Mk1 divertor. (b) Schematic of the Mk2A divertor. (c) Typical reconstructed poloidal section of the magnetic flux surfaces showing the last close flux surface and the strike zones of the scrape-off-layer plasma with the target plates. Viewing lines used for visible spectroscopic studies are superimposed for illustration.

Many diagnostic systems were upgraded and optimised prior to plasma operation with the Mk1 divertor (Breger and Vlases, 1991). As a result of the improved divertor

spectroscopy the JET MK1 divertor campaign has given the opportunity for detailed sets of observations of impurity atoms and ions and in some cases their molecular precursors. The geometrical complexity of the divertor plasma region, the localisation of power deposition flowing in the scrape-off-layer at the strike zones and divertor operational strategies, such as the creation of detached radiating plasma, presents a diagnostic challenge. The more common assumptions of homogeneous and/or equilibrium plasma as a vehicle for spectral interpretation are not sustainable. Rather it is necessary to link the spectral observations, divertor plasma models and the atomic modelling of the radiating plasma closely from the beginning. Multiple probes along the divertor target, tomographic bolometric reconstructions together with comprehensive wavelength spectroscopy along mutiple lines of sight through the divertor provide the experimental pulse data. In so far as each of these use derived atomic data, it is important for the integrated analysis that the various pieces of atomic data are consistent with each other, that is with the same fundamental data roots, to avoid confusion. A careful and structured approach to insertion of appropriate derived atomic parameters in this integrated task is, in these circumstances, enormously helpful. In these issues and anxieties, JET is typical of other fusion experiments such as ASDEX-upgrade, ALCATOR-Cmod, JT60 and DIIID.

In the next section of this paper, we review anecdotally our practical experience with a few of the important ions and species in divertor plasma and how the fundamental atomic data has impacted our studies of them. Then we consider some of the general aspects of the divertor, as a plasma in a dynamic and radiating state, must influence our approach. Finally, we discuss in some detail the building of appropriate atomic data sets and the generation of derived data from them, which are tuned to the actual models and diagnostic techniques we use for the divertor. It is hoped that these discussions, although built around our JET implemetation, are of general relevance to atomic physicists interacting with plasma physicists at other fusion experiments.

2. Studies of some impurities in divertors and the implications for the electron collision database

2.1. Helium at low temperature in gas puff experiments

Helium, as the major species in fusion reactors after the hydrogen fuel, is studied experimentally from its birth as fast alphas, through its cooling and thermalising in the high temperature core plasma to its exhaust in the cool divertor plasma. Then again, it has been used as a neutral species in heating beams providing at the same time a charge exchange and beam emission spectroscopic diagnostic. In the low temperature regime, it is electron collisions which excite and ionise helium and through such processes helium is an effective spectrum line radiator above 3-4eV. Because it has both singlet

and triplet spin systems and a high lying $1s2s\ ^3S$ metastable, it also has potential as a spectral line ratio diagnostic of electron temperature and electron density. Thus helium has become a popular species for study in the divertor, not only as a passive radiator but as a probe via active injection through a nozzle at thermal ($\sim$ .1eV) energies. The latter is a technique pioneered at TEXTOR (Brix et al.,1997; Schweer et al, 1992) and copied in most other laboratories. An experimental advantage is that suitable spectral lines for diagnostic line ratios lie in the visible. Relevant transitions are from the $n = 3$ to $n = 2$ shells on both the singlet and triplet sides. The effort to underpin the modelling of helium and diagnosis using its spectrum highlights the demands for atomic data, but also the sustained interaction between experimental spectroscopists, modellers and fundamental cross-section producers before a reliable diagnostic is created.

Electron impact collision cross-sections for helium, as the next simplest atom to hydrogen, have been evaluated many times and in many different approximations. It has become accepted that cross-section precision at the levels required for the above diagnostic applications ($\leq 20\%$) can only be met by close-coupling methods and particularly the R-matrix method (Burke and Berrington, 1993) - the most generally known and maintained technique. Successive R-matrix calculations over a period of years addressed increasing numbers of states - 19 state, 29 state etc. - so covering the $n = 3$ shell observed in fusion applications as well as higher shells relevant for cascade corrections. R-matrix calculations relate most strongly to the near threshold resonant region and have greater difficulty in the intermediate energy regime above the ionisation energy. Unfortunately, the fusion application needs rates in effect at all energies and so matching and merging of data are required. It is fortunate that de Heer (1996) has given very great and careful attention to this task, building a comprehensive data set from experimental cross-section measurements and theory. An important issue turned up. The R-matrix calculations were incorrect with successive efforts converging on the wrong values. The problem lay in the proximity of the continuum and simplification in its treatment. In the last two years or so, the converged close coupling work of Bray et al. (1994) has clarified this issue. It is now believed that the helium cross-sections are now truly well within the needed precision for fusion experiments. Recent experimental measurements of very detailed collision parameters for excitation to the $3d$ shell (Fursa et al.,1997) correspond closely with theory. Figure 2 shows a comparison of cross-section data for one transition prepared by de Heer and co-workers. The solid curve is the preferred (JET) cross-section. Maxwell averaged data are our main form of use. This complete collection of data for population modelling has been checked by Brix and is now used in the helium gas puff diagnostic. The behaviour of the diagnostic line ratios is shown in figure 3.

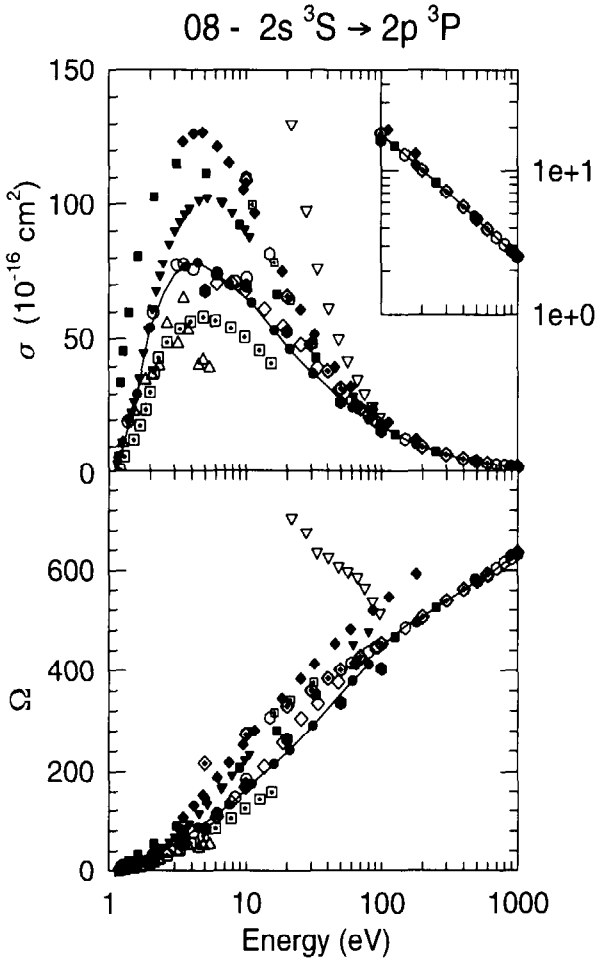

Figure 2. Comparison of various sources for the $HeI(2\ ^3S - 2\ ^3P)$ electron impact cross-section and collision strength.

2.2. Nitrogen and carbon emission in the VUV

During the JET MK1A divertor campaign with graphite target plates, experiments were carried out with nitrogen seeding to investigate the establishment and characteristics of a detached radiating divertor plasma. Figure 4 shows a typical VUV spectrum rich in lines of carbon and nitrogen ions. We are concerned with the distributions of the ions of these species in the divertor, their contribution to the radiated power from the divertor and their influx and recycling rates at the target surfaces. Because of the enhanced neutral hydrogen presence in the divertor region close to the targets it has

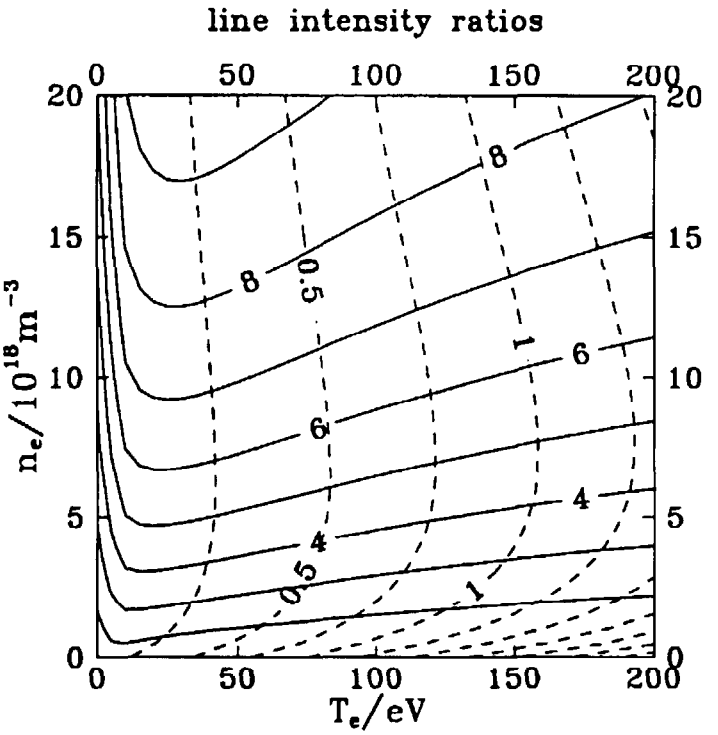

Figure 3. Some theoretical HeI line ratios as a function of electron temperature and electron density from Brix et al., 1997. Dashed line: T_e ratio $I(\lambda_1)/I(\lambda_3)$, solid line:$N_e$ ratio $I(\lambda_2)/I(\lambda_1)$. $\lambda_1 = 2\ ^1P - 3\ ^1S = 7281\mathring{A}$, $\lambda_2 = 2\ ^1P - 3\ ^1D = 6678\mathring{A}$ and $\lambda_3 = 2\ ^3P - 3\ ^3S = 7065\mathring{A}$

been a general expectation that charge transfer reactions involving neutral hydrogen will be influential on the ionisation state of impurities and on individual spectrum line emissions. It has been a task at JET to assess these items quantitatively. As regards charge transfer, our work to date has focussed mainly on the ions of carbon. Total charge transfer cross-sections and rates from ground state neutral hydrogen donors to change ionisation state have been available in tabulations from data centres such as ORNL for some years. To pursue a spectroscopic signature of charge transfer however it is in fact state selective charge transfer which is required. Such data has been less available. Typically, there have been some molecular calculations at very low energy motivated by astrophysical studies and experimental data at much higher energies, both outside the divertor conditions. At JET, Maggi (1997) (with assistance from Hoekstra) has assembled sets of state selective cross-sections for the carbon ions which represents the present situation. There has been quite substantial modification of our datasets

of this type over recent years. For example, for $C^{+3} + H(1s) \rightarrow C^{+2} + H^{+}$, which is of particular interest to us, we have been grateful to Herrero (private communication - 1996) for providing state selective data expanding on her earlier work (Herrero et. al., 1995). All these data merged with electron collision and other data are used in our divertor studies of carbon and have been circulated to a number of fusion laboratories.

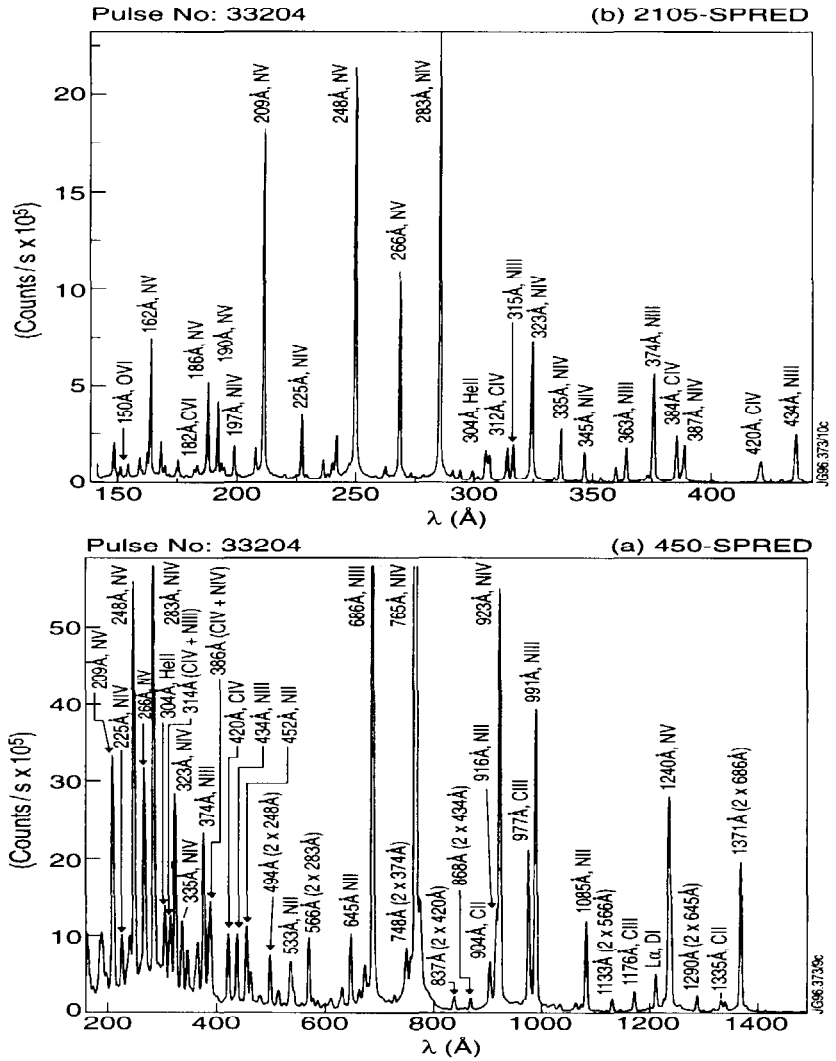

Figure 4. VUV spectra of the divertor from the 450-SPRED (a) and the 2105-SPRED (b) during a nitrogen seeded radiative divertor discharge (Pulse 33204)

For the low energy collisions typical of the divertor, the charge transfer is strongly state selective. For $C^{+3} + H(1s) \rightarrow C^{+2} + H^{+}$ only two states ($2p^2\ ^1S$ and $2s3s\ ^3S$) are strongly populated in the temperature range 1-10eV of relevance for the CIII spectrum

(see figure 5). In divertor plasma, direct charge exchange population of these levels competes with population by electron impact excitation by electrons from the ground and metastable levels of the C^{+2} ion. For representative neutral hydrogen densities ($N_H/N_e \leq 10\%$), the largest differential effect in line ratios from C^{+2}, when charge exchange is switched on and off, is $\leq 20\%$. This is well below the precision of measurements and the accuracies of the underlying cross-sections. Therefore it appears that for the carbon ions in JET MK1A divertor conditions, spectral line ratios from the same ion cannot be used as a charge exchange diagnostic in the same manner as they are used as electron temperature and density indicators. The next effect of charge exchange is the alteration of the overall carbon ionisation balance. This cannot be inferred immediately since the parallel flow of impurity ions along the open field lines in the divertor matters. The effective recombination and ionisation rates including the part from charge exchange must enter the plasma impurity model and be associated with the calculated neutral hydrogen distribution. It is found that the transport is hugely influential and that for JET conditions it masks almost completely the effect of charge transfer on the low ionisation stages of carbon. The matter is discussed more fully by Maggi in an associated brief presentation at this workshop. This result implies that the precise needs for arduous calculations of state selective charge transfer cross-sections must be carefully assessed.

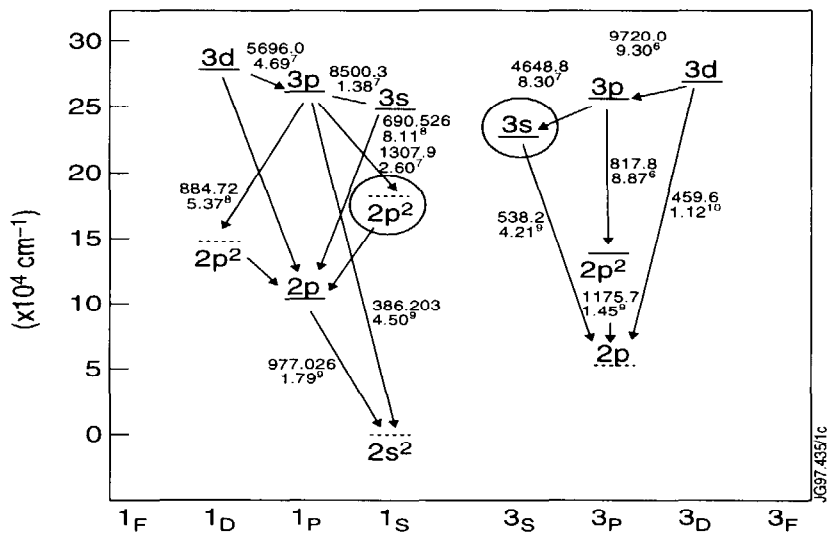

Figure 5. Grotrian diagram for C^{+2} with dominant CX receiving levels identified.

2.3. Molybdenum as an eroding target material

Heavy metals such as molybdenum and tungsten have desirable engineering and thermal resistance properties as divertor target materials countered by anxiety about their unfortunate efficiency as radiators if they enter the core plasma. Molybdenum is studied at ALCATOR Cmod as a divertor material and also at FTU (albeit as a limiter). The $z\ ^7P^o \rightarrow a\ ^7S$, $y\ ^7P^o \rightarrow a\ ^7S$ and $z\ ^5P^o \rightarrow a\ ^5S$ are observed at FTU (Gatti - private communication). It is common to infer influx of impurity neutrals such as molybdenum by measurement of the line-of-sight intensity of a single visible spectrum line and then dividing it by a theoretical photon efficiency. Note that for molybdenum, the ^7S is the ground state and ^5S the lowest lying metastable. Inference of flux by measurement of a spectrum line on the quintet side is a matter for caution. This is because the relaxation timescale for the metastable population may be such that equilibrium at the local temperature and density is not reached for the inflowing atom. Essentially it ionises too readily. The situation is illustrated in figure 6 where the population distributions of the metastables of Mo^{+0}, Mo^{+1} and Mo^{+2} are mapped at different times on entering a plasma of different electron temperatures.

Contrast the 1eV and 10eV results. For a 10eV plasma, we find that the ground ^7S and metastable ^5S term populations do not equilibrate until about $t = 4 * 10^{-6}\ s$. Note that the '7/5' population ratio only applies at high temperatures since at 1eV, the $exp(\Delta E(^5S - ^7S)/kT_e)$ factor is significantly larger than unity. However, by this time $(t = 4 * 10^{-6}\ s)$ we see also that the fractional abundance is dominated by Mo^+ and Mo^{+2}. Note that the Mo^+ populations are metastable resolved because of our final state resolved ionisation data but the Mo^{+2} are not. Thus for a 10eV divertor plasma, the radiation from the neutral occurs while the ^5S metastable term is not in equilibrium with the ^7S ground term. For a 1eV divertor plasma, we see that Mo is still the dominant ionisation stage at $t = 4 * 10^{-6}\ s$ where the ground and metastable terms equilibrate. Thus for such a plasma, the radiation emitted from the neutral is dominated by far by that emitted when the ^5S metastable term is in equilibrium with the ^7S ground term. From these results, which are also applicable to light influx atoms and ions, a metastable resolved picture of the evolution from ionisation stage to ionisation stage is required.

2.4. Argon as a divertor coolant

Argon has been of recent interest as a gaseous addition to the divertor plasma to enhance radiative cooling. Historic data on argon for transport modelling was highly simplified and some such as that at JET had been so little used that large un-noticed errors were present. Spectral observations of low stages of argon, especially of Ar^+ prompted enquiries from McCracken (1996 - private communication) at Alcator about photon efficiencies for certain lines. Also total radiated power needed to be reworked. Clark

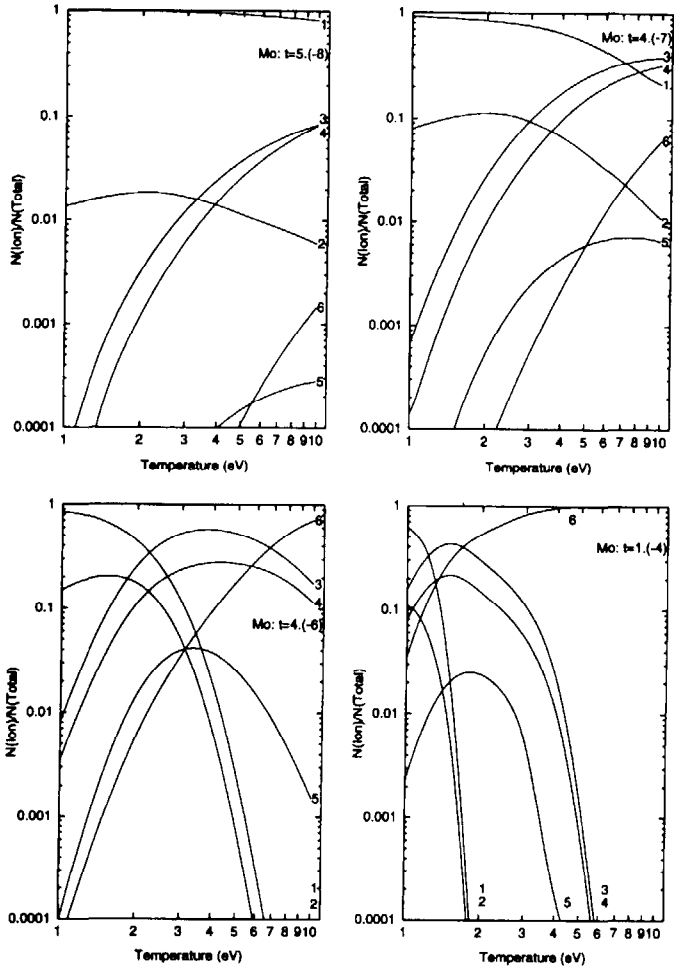

Figure 6. Population fractions for Mo at the times $t = 5 * 10^{-8}s$,$t = 4 * 10^{-7}s$, $t = 4 * 10^{-6}s$ and $t = 1 * 10^{-4}s$. Index 1, $Mo\ ^7S$; 2, $Mo\ ^5S$; 3, $Mo^+\ ^6S$; 4, $Mo^+\ ^6D$; 5, $Mo^+\ ^4D$; 6, Mo^{+2} *unresolved*

et al.(1995) used Los Alamos codes to generate a new equilibrium ionisation balance. At JET, we revisited argon with our baseline calculation. Simultaneously, Griffin et al. (1997) embarked on a detailed LS-coupled R-matrix calculation of electron impact excitation cross-sections for Ar^+. Griffin et al. also have a capability to calculate refined metastable resolved ionisation rate coefficients to match with the excitation data in determining photon efficiences. The calculations above are representative of the various levels of precision which can be brought to bear. The most sophisticated (Griffin et al.) are very consuming of computer time and feasible only for a few ions which must

be used as benchmarks. The variation between the approaches is shown in figure 7 for the total radiated power function in ionisation equilibrium. The low temperature region at $T_e \sim 3eV$ is to be noted. The R-matrix calculations confirm the distorted wave calculations (Clark et al., 1995) in this case. Total radiated power is, however, the least demanding theoretical quantity.

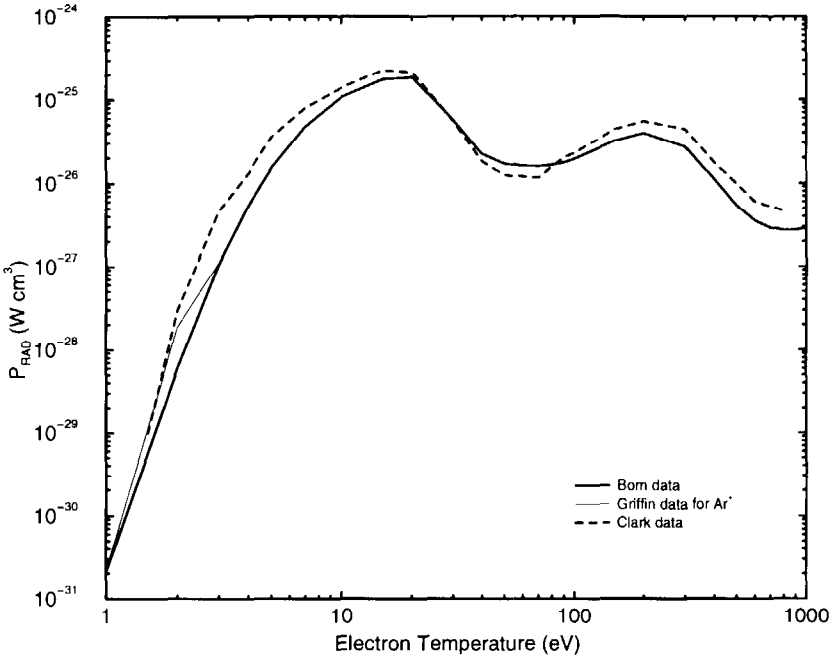

Figure 7. Argon radiated power function for static ionisation equilibrium.

3. Dynamic divertor plasmas

The divertor plasma is, by its very nature and purpose, one in which particles are in non-thermal flows in the scrape-off-layer, rising up the thermal gradients towards the bulk plasma, frictionally entrained in the primary plasma species flow into the divertor, impinging on surfaces, sputtered from surfaces or recyling from surfaces. All this within the geometries of the material boundaries of the divertor and the magnetic field lines in the divertor. Also the atoms and ions change state through ionisation and recombination and charge transfer with neutrals and their charge state (neutral or ion) determines the degree to which they are constrained by the magnetic field. The critical issue for the efficient introduction of atomic reactions into the complex fluid dynamic and particle dynamics is one of atomic versus plasma timescales.

3.1. Flows and dynamic ionisation

For the field geometry and physical conditions of selected pulses in the JET Mk1A divertor campaign, Maggi(1997) conducted model calculations of the distributions of deuterium ions, electrons, neutral deuterium atoms, and impurity ions. Such calculations allow an overview of relative time constants and the competing roles of transport, ionisation, charge exchange etc. In illustration, figure 8 shows some of these time constants for C^{+2} in the simulation of a high density, low temperature, ohmically heated discharge. Even in these conditions, the C^{+2} ion's population distribution is still dominated by ionisation, which is itself a consequence of the very strong parallel transport of the ion to higher temperature regions. In the region of overlap between the deuterium (donor) and C^{+3} (receiver) number density distributions, $\tau_{iz} \ll \tau_{cx}$, that is ionisation from C^{+2} into C^{+3} dominates over charge exchange recombination from C^{+3} into C^{+2} ions. This shows that, counter to expectations, charge exchange does *not* play an important role (cf. Maggi, this meeting) in the ionisation balance.

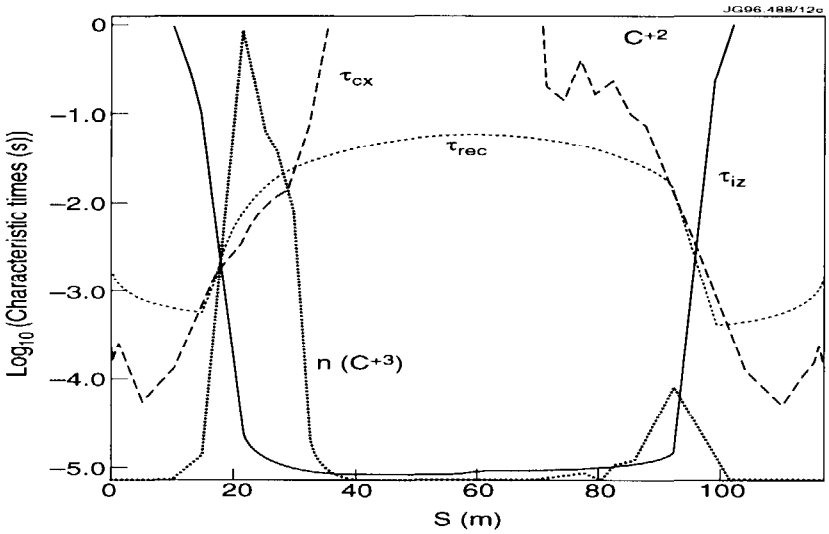

Figure 8. Characteristic times for C^{+2} along the separatrix ring, from the outer to inner target, for the simulation of a JET ohmic discharge at detachment. Overlayed is the normalised recombining C^{+3} ion density profile.

3.2. The collisional-radiative viewpoint

The above considerations indicate that our derived atomic calculations must be in the collisional-radiative framework. That is, as well as dealing with the mixture of collisional and radiative processes affecting population lifetimes, we must contrast atomic and

plasma transport timescales. Collisional-radiative theory provides the prescription for separating populations into those which are short lived, reflecting local conditions only and those which are long-lived, reflecting their past history. The former are small populations (the true excited state populations) which can be treated as quasi-static yet provide the spectral emission, while the latter are large and must enter the plasma transport equations explicitly. Generically, we call these large populations metastables. They include the ground populations of ionisation stages. Most plasma transport models, in fact, only include the ground state populations (or effectively the ionisation stage populations). The earlier illustrations in this paper indicate that the ground and low lying metastables are the 'correct' set of 'metastables' for a comprehensive picture. The production target of our collisional-radiative atomic modelling should be derived data relative to the complete set of metastables in the first instance, although it is perfectly reasonable to simplify further later, according to more specific conditions or available resources. From a practical point of view, the collisional radiative separation (we use the name 'generalised collisional-radiative' when we include the complete set of metastables) provides effective ionisation coefficients, effective recombination coefficients etc. which link metastable population to metastable population and then effective emission coefficients which give the spectral emission possible from the quasi-static populations once the metastable populations are known.

3.3. Modelling and analysing the JET divertor

The 'experimental' approach at JET to diagnostic study of the divertor is that of modelling observed signals and then comparing with the actual observed signals. Such an approach is almost mandatory for other than the simplest reductions of observed data because of the geometrical complexity of typical divertors. This has the disadvantage of requiring the use of the complete (or nearly complete) theoretical computational models of divertor fluid and particle transport (and their slow execution times) but with the advantage of allowing manipulation of relevant physical parameters of the models in seeking the simulation/observational match. This means that derived collisional-radiative atomic data enter the picture both in the form of source terms for the fluid and particle transport codes and as effective emissivity and radiant power data for the post-processing of the modelled ion distributions into simulated line-of-sight signals. A schematic of the JET approach is shown in figure 9. Such entry points, indicated as ADAS in the figure, are the final targets of all atomic data creation and all related atomic modelling of these atomic data into the derivative forms in fact used there. In the remainder of this paper we describe the acquisition, structuring and manipulation of atomic data to this end.

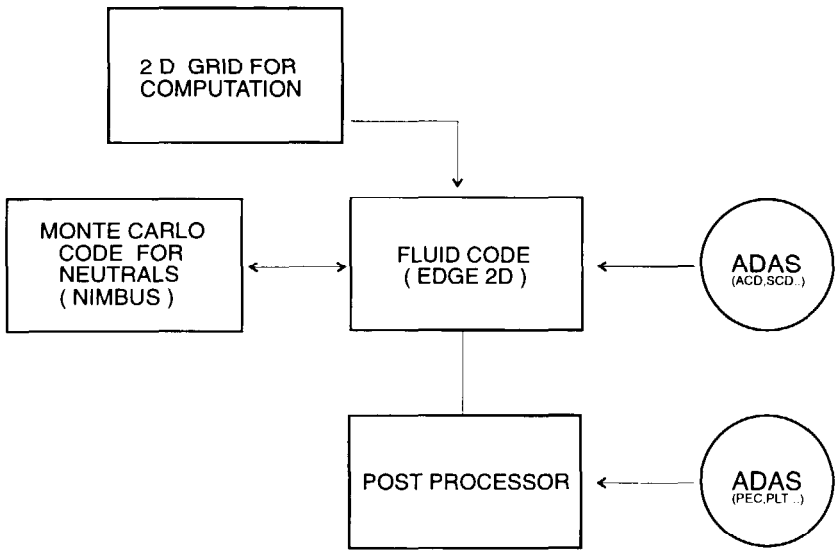

Figure 9. Schematic of the plasma modelling codes and post-processing used in simulating and analysing JET divertor signals. *2D grid*: from reconstruction of the magnetic equilibrium, generates a 2D field aligned net on which the computation is carried out. *Fluid code*: solve the 2D fluid equations for each species: electron, plasma and impurity ions (every charge state) are treated as species. *Monte Carlo code for neutrals*: particle, momentum, energy sources and losses for the plasma; neutral hydrogen isotope distributions, neutral impurity distributions. *Post−processor*: after the solution is obtained, performs integrations along diagnostic lines of sight of line emissivities, radiation profiles etc. *ADAS*: points of insertion of collisional-radiative atomic data.

4. Building and accessing the fundamental and derived databases

In this section, we wish to discuss in more detail the steps involved in building collections of fundamental atomic data which are in some senses complete for the divertor application. In describing these steps we shall use the JET system in illustration. It is called the 'Atomic Data and Analysis Structure', ADAS (Summers, 1994), and is available at some of the main fusion laboratories.

4.1. Electron collision datasets for divertor studies

For a given ion, for example N^{+0}, an initial decision is made of the set of energy levels which need to be addressed. This is primarily determined by the expected spectroscopy to be done on the ion. For most light divertor ions, we would hope to conduct visible and quartz UV as well as VUV spectroscopy and this means that energy levels up to the n=3 principal quantum shell must be included. The ground state of N^{+0} is $2s^2 2p^3\ ^4S$ but

we observe spectrum lines in the 'doublet' and well as the 'quartet' systems so doublet levels must be included. These must certainly include the $2s^2 2p^3\ ^2D$ and $2s^2 2p^3\ ^2P$ metastables since N^{+0} is an atom which may be in a transient state of ionisation with metastable populations not in static equilibrium with that of the ground state. For fusion applications, it is usually acceptable to deal with energy levels as whole LS terms rather than as J resolved levels in intermediate coupling. If there is a need to work in intermediate coupling then there is an immediate and substantial increase in the size of data structures. Nonetheless, with species such as N^{+0}, there is overlap of interest with astrophysical spectroscopy where J resolved studies are the norm. There is quite considerable trading of electron collision data between atomic physicists in the fusion and astrophysical areas and so within ADAS we have found it helpful to have a capability of transforming ion data sets between different 'resolution levels'.

Einstein A-coefficients are required for all allowed transitions between energy levels in the chosen set. Since we are including different spin systems and metastable levels, non-allowed spontaneous transitions need to be considered and it is sufficient to include only those which terminate on metastable states.

Then electron collision cross-sections between all energy level pairs must be incorporated. A usual assumption is that free electrons are Maxwellian and so it is Maxwell averaged rate coefficients rather than cross-sections which are included in the data structure. The Maxwellian assumption is doubtful in some divertor situations, but since detailed electron distribution functions are rarely if ever available, such points can be investigated by using superpositions of Maxwellians. Within ADAS, we store the Maxwell averaged rates in the normal course of events but in the form of the symmetrical,slowly varying, scaled quantity Upsilon, Υ, introduced by Seaton, which is now fairly universal. Incidentally, for true non-Maxwellian applications, it is appropriate to store the 'collision strength', Ω, rather than Υ, but then we must use an energy interval averaged $\bar{\Omega}$ since the true Ω has complex resonance structure. Typically tabulation of Υ at about twelve or thirteen electron temperatures or $\bar{\Omega}$ at about thirty energies covers all conditions.

Such an assembled dataset allows us to calculate the excited populations of levels of the ion relative to the ground level at any temperature and density. We have very many of such datasets, called *adf*04 files. Their layout is exactly prescibed (that is according to *a*DAS *d*ata *f*ormat 04). As they stand, however, they are incomplete for all divertor applications as they include no recombination, ionisation or charge transfer.

4.1.1. Adding free electron capture We seek to add free electron capture rate coefficients to each energy level of the set adopted for the ion. There are three parts to this, namely radiative recombination, dielectronic recombination and three-body recombination. The latter is the inverse of electron impact ionisation. In a

sophisticated formulation, radiative and dielectronic recombination occur as parts of one general process and can in principle interfere with each other. In practice, at least for light ions this is unimportant and radiative and dielectronic recombination can be treated as separate processes. Radiative recombination is obtained from the associated photo-ionisation cross-section via the Milne relation. If R-matrix photo-ionisation cross-sections are used which include resonances, then implicitly part of the dielectronic capture is added to the radiative recombination. This added part is not quite perfect since radiation damping of the resonances is not normally handled in R-matrix photo-ionisation cross-section calculations. However this is not a serious problem since regimes where the radiation damping matters can be isolated and treated separately as a dielectronic recombination calculation. Extended R-matrix photo-ionisation cross-section calculations have been carried out for astrophysics in the 'Opacity Project' (Seaton, 1987). Unfortunately, the only archived tabulations from these calculations do not resolve the final state of the photo-ionisation process. From the point of view of recombination, this means that the initial metastable from which recombination takes place is not identifiable. Thus the Opacity Project photo-ionisation data is not usable for our present purpose. Some re-computation of Opacity Project R-matrix photo-ionisation cross-section data with resolution of final state and then preparation of state selective radiative recombination coefficients has taken place for Be-like ions $\rightarrow$ B-like ions. This has been contrasted with simpler one-electron, effective potential calculations using the observed quantum defects. In cases when dielectronic recombination can be ignored agreement is very good (error $\leq$ 20%). It is our view that for fusion applications the latter method is entirely adequate. In ADAS, the *adf*04 datasets are extended with state selective radiative recombination coefficients for the designated set of energy levels at the same set of electron temperatures as for excitation rate coefficients. Note that at moderate to high temperatures, the predominant part of the overall radiative recombination takes place to low levels of the recombined ion which are usually spanned by the initial choice of level set. At very low temperatures, the contributions to radiative recombination from capture to higher n-shells increases but for purely hydrogenic rate coefficients are accurate to within a few per cent.

Dielectronic recombination presents a more substantial problem. There are an abundance of dielectronic recombination results in the literature but these are virtually all summed over final (recombined) states and are only for recombination from the ground state of the recombining ion. Also, dielectronic recombination coefficients are required not only to low levels in a resolved picture but also to very many higher n-shells. These data must be archived unsummed so that the modifications of the effective recombination due to redistribution and reionisation can be evaluated properly. It must be stressed that zero-density dielectronic calculations of total effective recombination, even though accurately done, are quite inappropriate for light ions at the typical densities

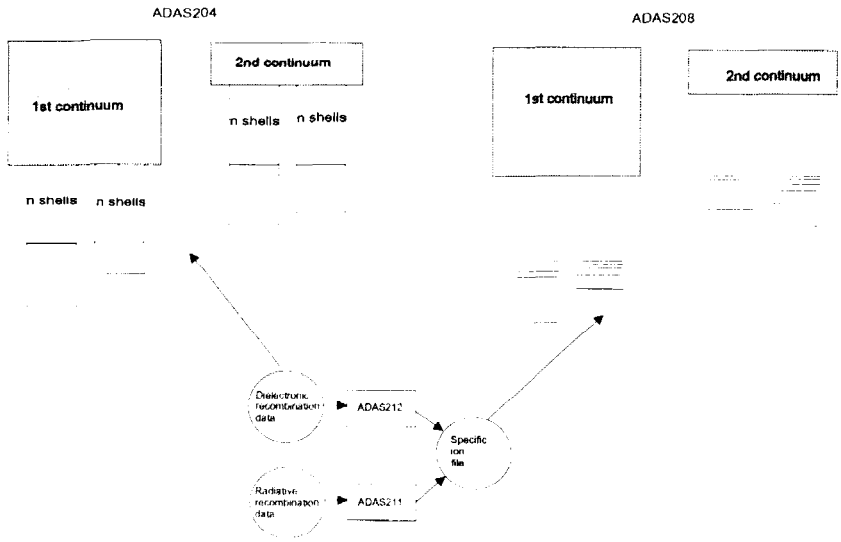

Figure 10. Schematic of mapping state selective radiative and dielectronic recombination coefficients to specific ion files.

of divertor plasma. With such large data flows involved, we have found it a great advantage to interact directly with those able to generate such dielectronic data. This is so that a detailed prescription of the data layout can be agreed which fulfills the fusion need prior to substantive calculations. Within ADAS, this corresponds to another data format, *adf*09. A dedicated code maps state selective dielectronic data from these very large collections onto the designated energy level set and adds it to the radiative part.

4.1.2. Adding charge exchange capture from hydrogen In divertor plasma, we must consider neutral atoms as electron donors which give another mechanism for recombination of impurity ions and a state selective process populating excited energy levels of an ion such as N^{+2}. Neutral hydrogen (or one of its isotopes) is the primary donor. The most important transfer may be from the ground or an excited level of the neutral hydrogen depending on the level of the recombined impurity to which the transfer occurs. For low energy collisions, that is at low ion temperatures, charge exchange is markedly state selective and sensitive to the fine detail of the intermediate molecule formed during the collision. There is not a large availability of such fundamental data and each dedicated calculation is time consumming. Unlike electron collisions, simple Maxwell averaged rate coefficients with the receiver assumed stationary are not realistic. The scenarios of the donor being beam-like (that is mono-energetic) and the receiver thermal, both donor and receiver being thermal but at different temperatures and a thermal donor with beam-like receiver are all credible in divertor modelling.

Thus archiving of state selective cross-sections rather than rates is appropriate. This means that algorithms which provide the required averaging over donor and receiver distributions must be executed according to circumstance. At JET, within ADAS, we use such codes to map from the cross-section archive onto our selected energy level set for an ion and append additional rate coefficient lines to the exisiting electron impact excitation, and recombination data of type *adf*04. After these various steps the specific ion file has the appearance shown in figure 11.

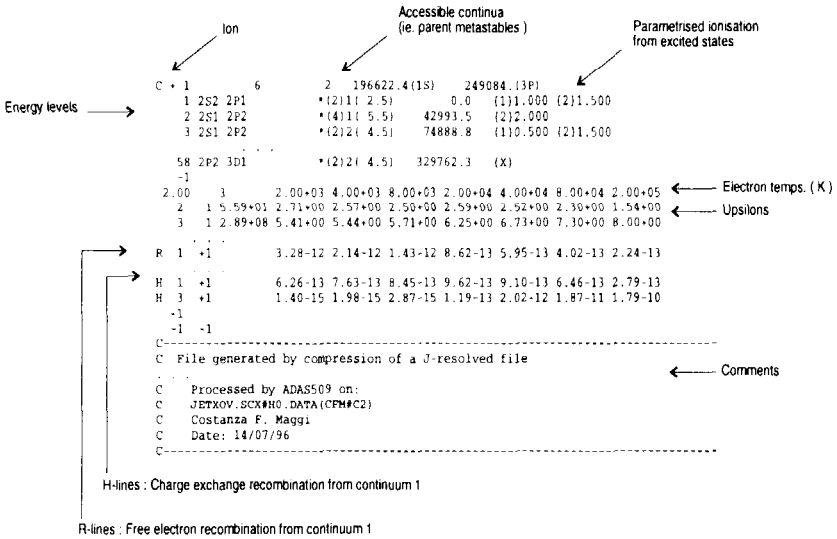

Figure 11. A portion of the specific ion (*adf*04) file for C^{+1} used in JET divertor studies. Note that the second part of the dataset consists of transition lines with the upper and lower energy level indices given first. The next column is used for the A-value for electron excitation lines and the remaining columns give Υ as a function of the electron temperature (in K) given at the head of each column. Recombination data and charge exchange data are indicated by the code letter 'R' or 'H' in the first character position of each row. Note that the data set has a substantial annotation section at its end which identifies the compiler of the different steps, the dates at which they occurred and a record of corrections and upgrades.

4.1.3. Adding the influence of higher n-shells Clearly data sets of the type described above are the focus of all the highest quality data which can be mustered in support of analysis using the ion in question. As such they may reflect very considerable effort by many people. The dataset however remains incomplete for study of the atomic properties since it includes only processes among the designated levels. For an ion in a low stage of ionisation in the relatively high densities and low temperatures of a divertor, populations of energy levels in for example the $n = 3$ shell of N^{+2} may also be

influenced by ionisation. Also this ionisation is not necessarily direct but may occur in a stepwise fashion through a series of higher excited n-shells. From the point of view of recombination when dielectronic recombination is active, a very substantial downward cascade of electrons from higher n-shells occurs which markedly alters populations and indeed contributes the bulk of the effective recombination in the collisional-radiative sense. Finally, even at low density, excitation from the ground level to higher n-shells followed by cascade gives a significant correction to that from direct excitation. The effects of higher n-shells must be included therefore to allow the precision obtainable in principle from the quality of the lower n-shell data. The estimation of the influence of higher n-shells may be calculated in simpler approximation since for such levels sub-shell mixing within an n-shell is very strong. At JET, we conduct such calculations within a parent and spin system resolved 'bundle-n' model and generate from it so-called 'projection matrices'. These are archived in the database and need not change as refinement of the low level data proceeds with time. Thus for the complete treatment of an ion, collisional-radiative population codes draw both upon the detailed specific ion file of type *adf*04 in ADAS and also upon the projection matrices (called *adf*17 in ADAS). Together, these datasets and the subsequent population calculations allow us to realise all the derived collisional-radiative data actually used in analysis and modelling. For us, such datasets are the structures into which we seek to meld disparate fundamental data from many sources.

4.2. Creating and channelling effective coefficients

For modelling and spectral analysis of the divertor, we have found it necessary to prepare a number of types of derived datasets. These fall into two classes. The first class is required to establish the distribution of impurity ions in the divertor. These data are used by the impurity transport models. The second class is that of derived data required to interpret the radiation losses from the plasma. These include total radiated power at the grossed-up end of the scale and emissivities of specific lines at the other. Also, for quick inferences of impurity influx and emission shell shapes, one or two other forms of derived data are usually created. Such data can allow either eduction of the calibrated observed photon counts to physical quantities or can enter simulation of the spectrometer signals for matching with observation. These are summarised in the table below.

The various derived data sets summarised above are each functions of plasma electron temperature and plasma electron density. Also they are metastable resolved. Thus the effective recombination coefficient for $C^{+2} \rightarrow C^{+1}$ has separate parts for $2s^2\ ^1S \rightarrow 2s^2 2p\ ^2P$, $2s2p\ ^3P \rightarrow 2s^2 2p\ ^2P$ and $2s2p\ ^3P \rightarrow 2s2p^2\ ^4P$. We call these the generalised collisional-radiative coefficients. In our progressive refinement of this type

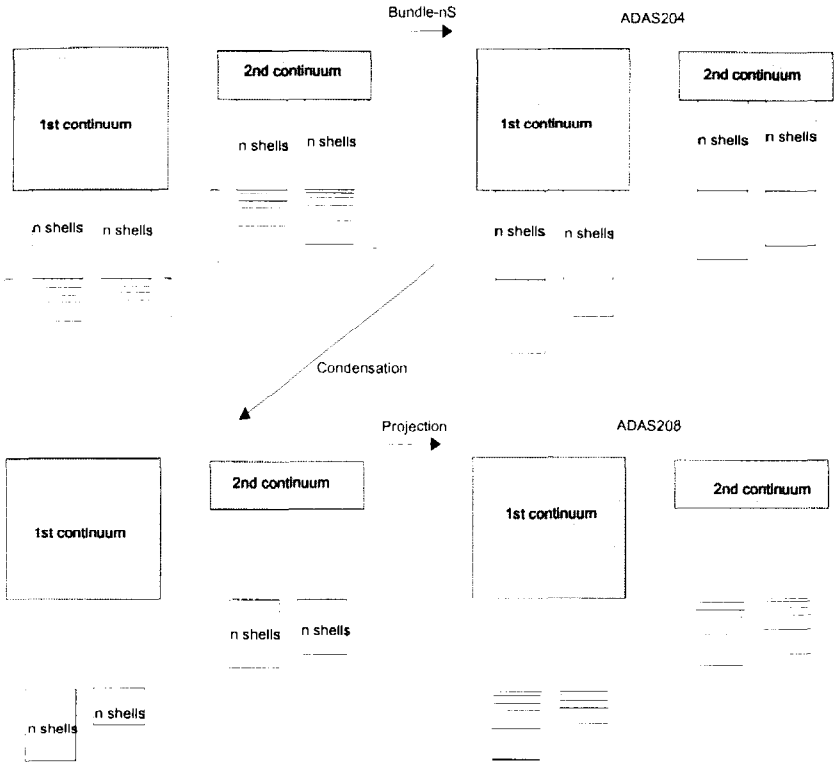

Figure 12. Schematic of bundle-n population calculation and the condensation and mapping to the low level set of the specific ion file.

adf type	Subcode	Content
adf11	acd	generalised collisional-radiative recombination coefficient
adf11	scd	generalised collisional-radiative ionisation coefficient
adf11	ccd	generalised collisional-radiative CX recomb. coefficient
adf11	qcd	generalised collisional-radiative cross-coupling coefficient
adf11	xcd	generalised collisional-radiative parent cross-coupling coefficient
adf11	prb	generalised collisional-radiative recomb/bremss. power coefficient
adf11	plt	generalised collisional-radiative low-level line power coefficient
adf11	prc	generalised collisional-radiative CX recom. power coefficient
adf11	pls	generalised collisional-radiative specific line power coefficient
adf11	met	generalised collisional-radiative metastable fractions
adf13	sxb	ionisation per photon coefficients
adf15	pec	photon emissivity coefficients

Table 1. Definition of ADAS derived datasets used in divertor modelling

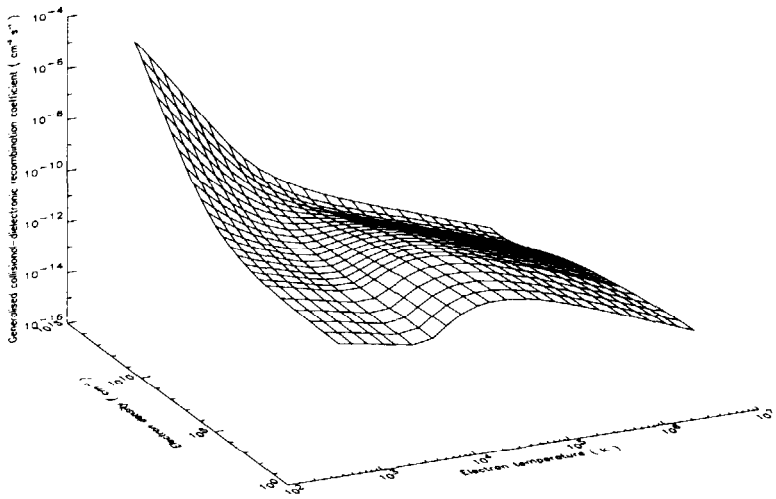

Figure 13. Generalised collisional-radiative recombination coefficient for $C^{+2}_{2s^2\ {}^1S} + e \rightarrow C^{+1}_{2s^2 2p\ {}^2P}$. This is the ground state to ground state part of the metastable resolved data. Note the high density three-body regime at low temperatures and the suppression of the high temperature dielectronic part at higher densities before three-body recombination takes over.

of data, we have now moved to tabulations at the fairly dense grid of temperature and densities shown in figure 13. Note that in practice the tabulation of data for members of the same isoelectronic sequence is made at z-scaled temperatures and densities.

The level of complexity involved in metastable resolution certainly matters for ionisation stages which are targetted for spectroscopic diagnostic use, but may be excessive for less important ionisation stages and simpler modelling. This is especially true for heavy species with many ionisation stages. To allow practical computations with reasonable execution times and storage requirements, it is helpful to reduce the effective number of populations (stages, grounds or metastables) to be handled. We have found it useful to arrange our primary storage of metastable resolved collisional-radiative data by isoelectronic sequence as indicated above. A separate computational step then gathers together those ions from the iso-electronic sequence archives to assemble an iso-nuclear sequence (that is the data for a particular element). This gathering step can simultaneously implement a condensation of the data in a manner tuned to the intended use. A schematic is shown in figure 14. We define a partition of the complete list of metastable states which specifies a grouping. The metastable resolved equilibrium ionisation balance can be used to decide the proportions to be used in generating a

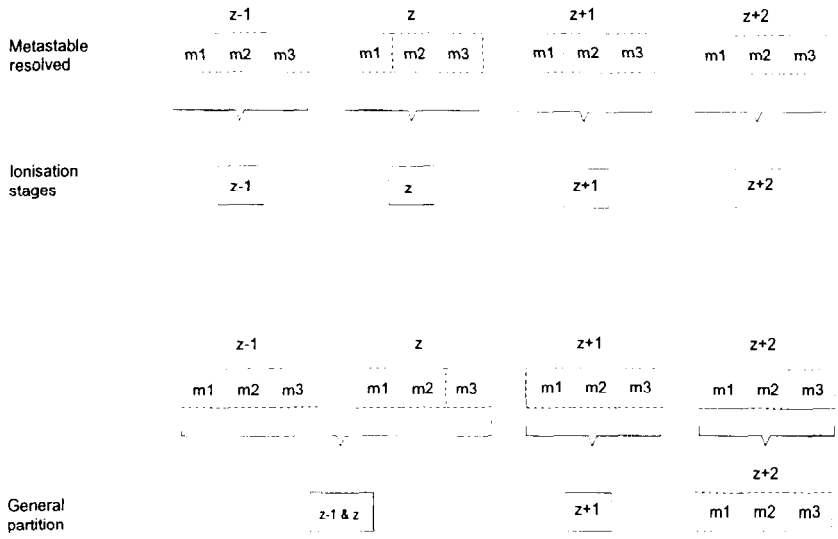

Figure 14. Schematic of flexible partitioning and condensing of metastable resolved collisional-radiative coefficient data as appropriate for the modelling and analysis.

new condensed set of collisional-radiative data linking partition member to partition member. The simplest condensing partition is to combine metastables belonging to the same ionisation stage. Such a condensation restores the usual stage to stage data but with a sounder pedigree. At JET for light ions we have worked mostly with the fully metastable resolved partition and the stage partition.

5. Discussion and conclusions

It is evident that a degree of balance is required in declaring a need for electron and neutral collision data for divertor. A few atoms and ions, such as He^{+0}, are very valuable diagnostically and merit considerable effort in generating the fundamental data for them. For many others, a lower quality is acceptable until a need for high precision data is really demonstrated experimentally. Thus, for example, our work with state selective charge exchange in carbon does not at this stage justify a demand for the highest quality close-coupled molecular calculations for other species such as nitrogen.

In actual use of data in analysis of spectral emission from low temperature plasma, it is always difficult to judge whether discrepancies arise from uncertainties in the plasma description or in the fundamental data. It does seem that, in our experience, nominally high quality theoretical cross-section data may be significantly less reliable than indicated by the notional precision of the method.

At the medium quality level, mass production codes are enormously helpful in setting

up a broad basis of description. However, in the light of the extensive collisional-radiative modelling necessary for the divertor, it is essential that the data be structured and organised from the beginning for entry into such models. Our most marked progress has been made when we have agreed *in advance* with the source producers of fundamental data exactly what data should be output and how it should be laid out. In this context, it is self-consistent collections of data, complete for the identified task, which are most useful.

We have frequently found it very hard work to merge data of different code origins. Some agreement to modest adjustments at the generation and output stages could make such tasks very much easier.

References

Breger P and Vlases G 1991 *JET Joint Undertaking Report* JET-TN(91)04

Badnell N R, Gorczyca T W, Pindzola M S and Summers H P 1996 *J. Phys. B* **29** 3683

Bray I, Fursa D V and McCarthy I E 1994 *J. Phys. B* **27** L423

Brix M and Schweer B 1997 *24th Eur. Phys. Soc. Conf. - Control. Fusion and Plasma Physics* **P4.116** 545

Burke P G and Berrington K A 1993 *Atomic and Molecular Processes: An R-matrix Approach* (IOP Publishing Ltd.)

Clark R, Abdallah, J and Post D 1995 *J. Nucl. Materials* **120-122** 1028

Fursa D V, Bray I, Donnelly B P, McLaughlin D T and Crowe A 1997 *J. Phys. B* **30** 3459

Griffin D C, Pindzola M S, Shaw J A, Badnell N R, Summers H P and O'Mullane M 1997 *J. Phys. B* **30** 3543

de Heer F J, Bray I, Fursa D V, Bliek F W, Folkerts H O, Hoekstra R and Summers H P 1996 *Atomic and Plasma Material Interaction Data for Fusion* **6** et al.

Herrero B et al 1995 *J. Phys. B* **28** 4607

Maggi C F M 1997 *Ph.D. Thesis* University of Strathclyde

Schweer B, Mank G, Pospieszczyk A, Brosda B, Pohlmeyer B, 1992 *J Nucl Mat* **196-198** 174-178

Seaton M J 1987 *J. Phys. B* **20** 6363

Summers H P 1994 *Atomic Data and Analysis Structure* JET Joint Undertaking Report JET-IR(94)06; *http : //patiala.phys.strath.ac.uk/adas/*

List of Figures